

ORIGINAL ARTICLE

MOLECULAR ECOLOGY WILEY

Functional colour genes and signals of selection in colour-polymorphic salamanders

James D. Burgon¹ | David R. Vieites² | Arne Jacobs¹ | Stefan K. Weidt³ |
 Helen M. Gunter⁴ | Sebastian Steinfartz⁵ | Karl Burgess³ | Barbara K. Mable¹ |
 Kathryn R. Elmer¹

¹Institute of Biodiversity, Animal Health & Comparative Medicine, College of Medical, Veterinary and Life Sciences, University of Glasgow, Glasgow, UK

²Museo Nacional de Ciencias Naturales (MNCN), Consejo Superior de Investigaciones Científicas (CSIC), Madrid, Spain

³Glasgow Polyomics, Wolfson Wohl Cancer Research Centre, College of Medical Veterinary and Life Sciences, University of Glasgow, Glasgow, UK

⁴Edinburgh Genomics, King's Buildings, University of Edinburgh, Edinburgh, UK

⁵Department of Evolutionary Biology, Unit Molecular Ecology, Zoological Institute, Technische Universität Braunschweig, Braunschweig, Germany

Correspondence

Kathryn R. Elmer, Institute of Biodiversity, Animal Health & Comparative Medicine, College of Medical, Veterinary and Life Sciences, University of Glasgow, Glasgow, UK.

Email: Kathryn.Elmer@glasgow.ac.uk

Present address

Arne Jacobs, Department of Natural Resources, Cornell University, Ithaca, NY, USA
 Sebastian Steinfartz, University of Leipzig, Institute of Biology, Molecular Evolution and Systematics of Animals, Leipzig, Germany
 Karl Burgess, Institute of Quantitative Biology, Biochemistry and Biotechnology, School of Biological Sciences, University of Edinburgh, Edinburgh, UK

Funding information

Royal Society, Grant/Award Number: RG130800; Wellcome Trust, Grant/Award Number: 105614/Z/14/Z; Natural Environment Research Council, Grant/Award Number: NE/L501918/1; Ministerio de Ciencia e Innovación, Grant/Award Number: CGL 2017-89898-R

Abstract

Coloration has been associated with multiple biologically relevant traits that drive adaptation and diversification in many taxa. However, despite the great diversity of colour patterns present in amphibians the underlying molecular basis is largely unknown. Here, we use insight from a highly colour-variable lineage of the European fire salamander (*Salamandra salamandra bernardezi*) to identify functional associations with striking variation in colour morph and pattern. The three focal colour morphs—ancestral black-yellow striped, fully yellow and fully brown—differed in pattern, visible coloration and cellular composition. From population genomic analyses of up to 4,702 loci, we found no correlations of neutral population genetic structure with colour morph. However, we identified 21 loci with genotype–phenotype associations, several of which relate to known colour genes. Furthermore, we inferred response to selection at up to 142 loci between the colour morphs, again including several that relate to coloration genes. By transcriptomic analysis across all different combinations, we found 196 differentially expressed genes between yellow, brown and black skin, 63 of which are candidate genes involved in animal coloration. The concordance across different statistical approaches and ‘omic data sets provide several lines of evidence for loci linked to functional differences between colour morphs, including *TYR*, *CAMK1* and *PMEL*. We found little association between colour morph and the metabolomic profile of its toxic compounds from the skin secretions. Our research suggests that current ecological and evolutionary hypotheses for the origins and maintenance of these striking colour morphs may need to be revisited.

This is an open access article under the terms of the Creative Commons Attribution License, which permits use, distribution and reproduction in any medium, provided the original work is properly cited.

©2020 The Authors. *Molecular Ecology* published by John Wiley & Sons Ltd.

KEYWORDS

amphibian, coloration, colour candidate genes, gene expression, genetic architecture, genomic association, population genomics, response to selection, toxicity

1 | INTRODUCTION

Animal coloration is conspicuously affected by natural and sexual selection (Caro, 2005) and therefore is an ideal system in which to study the evolutionary processes that generate and maintain biological diversity (Andrade et al., 2019; Barrett et al., 2019; Harris et al., 2020; Hubbard, Uy, Hauber, Hoekstra, & Safran, 2010; Kusche, Elmer, & Meyer, 2015; Stevens & Ruxton, 2012). Within the terrestrial vertebrates, amphibians present some striking colour patterns that vary both within and across species and are often presumed to be associated with ecological and physiological functions (Cott, 1940; Thayer, 1909). For example, putative antipredator strategies that are based on colour include crypsis or disruptive coloration (concealment through background colour matching or camouflage by pattern) and aposematism (an interspecies warning coloration communicating toxicity or unpalatability; Kerr, 1919; Ruxton, Sherratt, & Speed, 2004). Colour variation may also be associated with thermoregulation and water loss reduction (Duellman & Trueb, 1994; Moore & Ouellet, 2015; Rudh & Qvarnström, 2013), for example as suggested by an observed increase in melanistic morphs at high altitudes and latitudes (Alho et al., 2010; Vences et al., 2002, 2014). However, inferences about the selective pressures that generate and maintain colour polymorphisms in amphibians have often been speculative and correlational, and the molecular underpinnings poorly understood (Hoffman & Blouin, 2000; Rudh & Qvarnström, 2013).

The ecological and evolutionary genomics of amphibians has been somewhat impeded by logistical and biological complications compared to the rapid recent advances in mammals, fish and birds (McCartney-Melstad, Mount, & Shaffer, 2016; Rudh & Qvarnström, 2013). For example, the challenges of captive breeding hamper genetic mapping for quantitative traits, especially in those species that have internal fertilization, long-term sperm storage, lengthy gestation times and small clutch sizes (Rudh & Qvarnström, 2013). Second, in many cases the colour variations are among species rather than within, which hinders distinguishing genomic patterns associated with colour rather than species differences. Third, amphibians have very large genome sizes, ranging up to 121 pg (Gregory, 2019), which has slowed the pace of reference genome development and functional genomic analyses compared to other vertebrates (Koepfli, Paten, & O'Brien, 2015). Large genome size in salamanders is due to an excess of repetitive elements but the size and number of coding genes is similar to that of other vertebrates (Nowoshilow et al., 2018). To advance knowledge of how selection affects the origins and maintenance of amphibian colour variation, analyses of colour polymorphisms and related genetic patterns in environmental context are needed.

Here, we provide novel insights into the genetic basis of coloration in amphibians using a highly colour-polymorphic lineage of salamander. Fire salamanders (subspecies in *Salamandra atra*) have an array of yellow, black, brown, red, orange, white, striped and spotted colorations that are usually fixed within subspecies (Sparreboom & Arntzen, 2014; Thiesmeier, 2004; Thorn & Raffaelli, 2001). The striking colour patterns are widely assumed to be aposematic, functioning as warning coloration (Beukema, Speybroeck, et al., 2016). Fire salamanders are able to release endogenously produced noxious secretions from their enlarged paratoid glands at the base of the head and smaller glands along the spine as an antipredator defence, which are quite toxic compared to those of most European amphibians (Lüddecke, Schulz, Steinfartz, & Vences, 2018; Trochet et al., 2014; Vences et al., 2014). Alternatively but nonexclusively, the black and bright spotted or striped coloration may act as a form of concealment in forested habitats, as aposematic coloration can also be visually disruptive (Stuart-Fox & Moussalli, 2009), although this has yet to be empirically tested. Some *Salamandra* lineages have evolved melanistic colorations by losing the yellow components (Bonato & Steinfartz, 2005; Steinfartz, Veith, & Tautz, 2000; Vences et al., 2014). This is presumed to be due to selection for thermoregulation because, being ectotherms, darker skin at higher altitudes protects against ultraviolet light and enables more efficient warming from the sun. Repeated independent evolution of melanistic and striped morphs and sister lineages at higher altitude are suggestive evidence for this hypothesis (Beukema, Speybroeck, et al., 2016; Lüddecke et al., 2018; Rodríguez et al., 2017; Vences et al., 2014). Maintenance of colour morphs within a population might be promoted by colour-based assortative mating, as proposed in other salamanders (Acord, Anthony, & Hickerson, 2013), but not yet tested in this species. Aposematism, crypsis, thermoregulation and assortative mating have been demonstrated to different extents in colour polymorphism generation and maintenance at the phenotypic level but to date have been rarely evaluated in a salamander.

In this study we aimed to identify if signals of response to natural selection are associated with coloration in colour- and pattern-variable salamanders. Experimentally we used a lineage of fire salamanders that have striking solid-coloured yellow and brown colour morphs and intermediate colorations alongside the more typical ancestral yellow-black striped morph (Beukema, Nicieza, Lourenço, & Velo-Antón, 2016; Köhler & Steinfartz, 2006; Figure 1). Our expectation is that functional genomic variation differs between colour-polymorphic phenotypes and there are genomic signals of response to selection. We: (a) characterized coloration for pattern, visible and nonvisible colour, and cellular

structures; (b) associated genome-wide genetic variation with colour morph and inferred signals of selection on genomic patterns; (c) identified functional candidate genes for coloration based on expression; and (d) assessed the intersections between genome-wide association, functional expression and signals of selection. Using this, we evaluated support for three major standing hypotheses for the existence of colour morphs: local adaptation to altitudinal differences, assortative mating and differential antipredator toxins (Acord et al., 2013; Beukema, Speybroeck, et al., 2016). The coexistence of different colorations within a single environment offers a natural experiment for inferring genetic bases, ecological and phenotypic correlates of colour, and disentangling response to selection.

2 | METHODS

2.1 | Field sampling

Adult salamanders were sampled at seven localities in Asturias, Spain, from 78 to 1,312 m asl (Figure 1). Striped individuals were found at all sites; brown and yellow salamanders were found at localities 4–7. Gradations between striped, yellow and brown also exist in the population but our sampling focused on characterizing the most representative colorations. Standardized dorsal images were taken using a Canon EOS 70D DSLR camera using a 100-mm lens and with an X-Rite ColorChecker. Tissue samples (toe or tail clips) were stored

in ethanol. Salamanders were released where captured, except those representatives sampled for microscopy and gene expression studies. Sex was inferred from cloacal swelling in males.

2.2 | Colour pattern analysis

While salamanders can be clearly grouped into colour morph by eye, colour patterns were additionally examined objectively and quantitatively from a single densely sampled colour polymorphic sample site (Site 7) to mitigate any interpopulation effects. Photographs were standardized in Adobe Photoshop CS6: (a) a custom camera profile (generated using X-Rite's DNG ProfileManager) was applied, (b) the white balance of each image was set using the white square of the X-Rite ColorChecker, and (c) the exposure was modified until the RGB (red, green and blue) values of the white ColorChecker square equalled 240:240:240 (± 5). Dorsal colour patterns were analysed in R (R Core Team, 2013) using *Patternize* (Van Belleghem et al., 2018). Only clear images without obvious body contortions were used: 61 striped, 115 yellow and 44 brown (total $N = 220$). The ratio of females to males per colour morph was 1.3, 1.3 and 1.6 respectively. Image registration and colour pattern extraction was carried out using the *patRegK* function. The *patPCA* function was used to conduct principal component analyses (PCAs) to look at differences between the three colour morphs. Resulting PC scores were compared via one-way ANOVA.

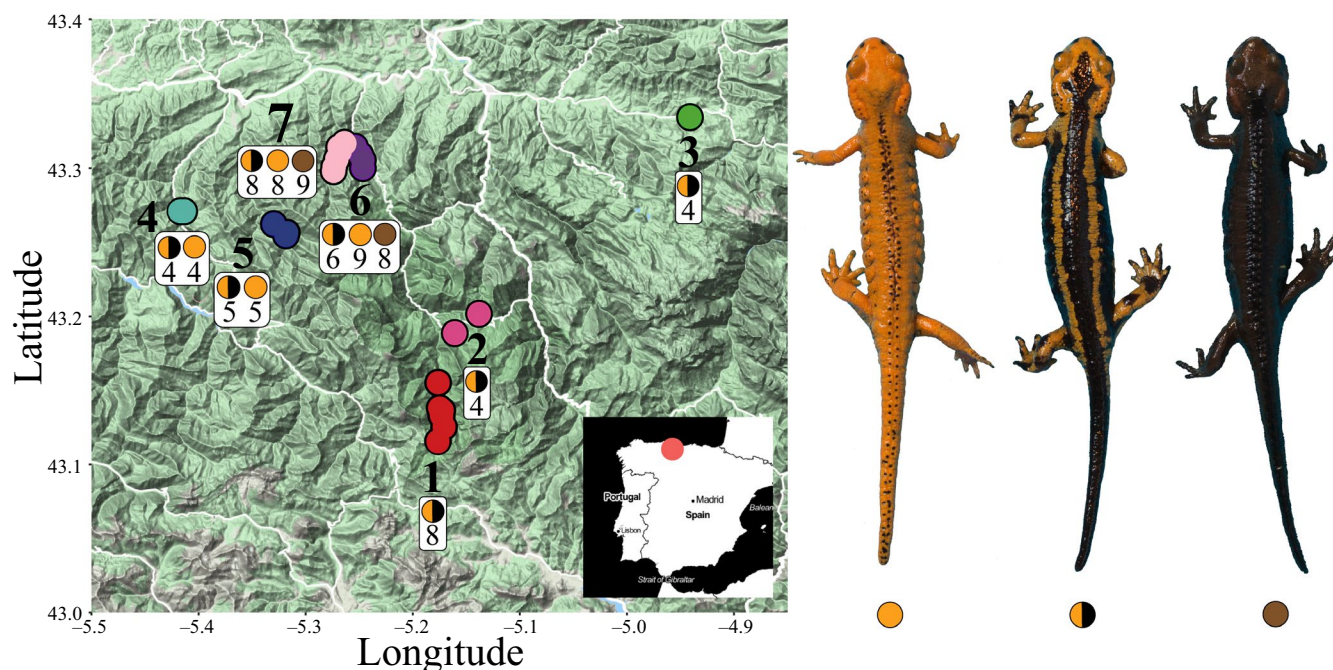


FIGURE 1 Colour morphs and sample site locations in Asturias, northern Spain: 1 (red) Ventaniella-Soberfoz; 2 (magenta) San Juan de Beleño; 3 (green) Avín; 4 (turquoise) La Marea; 5 (blue) Rio del Infierno; 6 (purple) Tendi valley; and 7 (light pink) Rio Color. Sites 1–3 are monomorphic ("striped-only"); sites 4–7 are colour-polymorphic. The number of individuals of each colour morph ddRAD-Seq genotyped from each sample site is also shown (striped, yellow, or brown circles). Inset: the broader geographical location of the sample region (red square). Base map: Google Maps [Colour figure can be viewed at wileyonlinelibrary.com]

2.3 | Reflectance spectrophotometry

Three independent reflectance spectrophotometry readings were taken from seven morphology points to characterize coloration in the three morphs: the centre of the head, left paratoid gland, dorsal, lateral, gular and ventral landmarks (Figure S1a) ($N = 4$ striped, 10 yellow and 10 brown; F:M = 1.5, 0.43 and 3.0 respectively) using an Ocean Optics USB2000 Miniature Fiber Optic Spectrometer, a DHU 2000 Deuterium Tungsten Halogen Light, an Ocean Optics ZR100UUV/SR seven-fibre probe, a white Spectralon diffuse reflectance standard and Ocean Optics SpectraSuite software. A custom probe sheath was made to take measurements from a distance of 1 mm at an angle of 90° . Spectra were truncated to 300–750 nm and averaged per landmark per individual using the R package PAVO (Maia, Eliason, Bitton, Doucet, & Shawkey, 2013). A lamp artefact between 654 and 660 nm was manually removed. Hue values for each landmark per colour morph were analysed with one-way ANOVA.

2.4 | Transmission electron microscopy (TEM)

To identify the chromatophores that underlie different skin colours, two dorsal skin samples were dissected from striped, yellow and brown salamanders (Figure S1b; $N = 2$ individuals per colour morph). Sample processing followed established protocols (e.g. Graham & Orenstein, 2007). Briefly, skin samples were: (a) fixed for 2 hr using 2.5% glutaraldehyde in 0.1 M sodium cacodylate buffer, (b) rinsed with 0.1 M sodium cacodylate buffer, (c) postfixed in 1% osmium tetroxide, (d) stained in 0.5% aqueous uranyl acetate, (e) dehydrated in graded concentrations of ethanol and (f) embedded in Araldite epoxy resin. Using an ultratome, semithin (0.5–1 μm) sections were cut and stained with 0.5% toluidine blue for light microscopy, and ultrathin sections (60–70 nm) were cut and stained with 0.5% aqueous uranyl acetate and lead citrate for TEM imaging on an FEI Tecnai T20 electron microscope (University of Glasgow, Kelvin Nanocharacterisation Centre).

2.5 | Metabolomics of toxin

We investigated the relationship between colour phenotype and the metabolomic content of the toxic secretions using gas chromatography–mass spectrometry (GC-MS). The highly viscous secretions of six striped (0.5 M:F), six yellow (1 M:F) and six brown (1 M:F) salamanders (from Sample Site 7) were directly expressed into collection tubes by gently squeezing the left paratoid gland. An outgroup subspecies, *S. s. terrestris*, was included for comparison ($N = 6$). The weight of each sample was determined and a ratio of 5 mg secretion to 200 μl of ice-cold chloroform/methanol/water (1:3:1) used to extract metabolites by vortexing at 4°C for 5 min and centrifuging at 13,000 g and 4°C for 3 min; the supernatant (~90% of the solvent used) was then isolated and stored at -80°C .

The GC-MS analysis was performed at Glasgow Polyomics. First, 30 μl of each chloroform/methanol/water secretion extract were dried in a SpeedVac for 30 min, then 50 μl MSTFA + 1% TMCS was added to each and sealed. Samples were vortexed for ~10 s and incubated at 80°C for 15 min. Samples were cooled to room temperature, then 1 μl of each sample was injected into a Split/Splitless (SSL) injector at 250°C using a splitless surge injection on to a TraceGOLD TG-5SILMS (30 m \times 0.25 mm \times 0.25 μm) (Thermo) column installed in a Trace Ultra GC gas chromatograph. The initial temperature was 40°C , followed by a gradient of $30^\circ\text{C}/\text{min}$ ramp rate. The final temperature was 330°C and held for 4 min. Eluting peaks were detected via an ITQ900-GC mass spectrometer (transfer temperature 250°C , 60–800 m/z). Ions were generated using chemical ionization with a methane reagent gas (1.5 ml/min, source temperature 180°C , emission current 50 μA). Known *Salamandra* alkaloids were identified by comparing mass spectra and GC retention times with known data (Mebs & Pogoda, 2005). A PCA was carried out on the intensities (abundance) of identified metabolite peaks in the R package *mixOmics* (Cao et al., 2017). One-way ANOVA comparisons were made for each peak between: (a) the three colour morphs and (b) all *S. s. bernardezi* versus the outgroup *S. s. terrestris*.

2.6 | ddRAD sequencing, *de novo* assembly and quality control

Genomic DNA was extracted from 82 individuals collected across all sample sites (Figure 1; $N = 4$ –25 per site) using the Macherey-Nagel NucleoSpin Tissue kit. A double digest restriction site associated DNA sequencing (ddRAD-Seq; Peterson, Weber, Kay, Fisher, & Hoekstra, 2012) library was then prepared as follows (per Recknagel, Jacobs, Herzyk, & Elmer, 2015, with modification of Illumina adapters): (a) 1 μg of DNA from each individual (plus six technical replicates) was double-digested using the *Pst*I-HF and *Acl*I restriction enzymes (New England Biolabs); (b) modified Illumina adaptors with unique barcodes for each individual were ligated to the DNA; (c) samples were multiplexed; (d) a PippinPrep (Sage Science) was used to size-select fragments around a tight selection of 383 bp (range: 350–416 bp) based on the length distribution visualized using a 2,200 TapeStation (Agilent Technologies); and (e) enrichment PCR was performed to amplify the library using forward and reverse RAD primers. Sequencing was conducted on an Illumina NextSeq 500 platform (865 million reads) at Glasgow Polyomics, generating paired-end reads 75 bp in length.

Raw sequence reads were quality checked using FASTQC version 0.11.3 (Andrews, 2010). The STACKS version 1.44 (Catchen et al., 2011) *process_radtags* pipeline was then used to demultiplex samples, remove Illumina adaptors and barcodes, and truncate reads to 60 nt. The cut site was then checked using the FASTX-TOOLKIT (*fastx_barcode_splitter.pl*; Gordon & Hannon, 2008). Processed reads averaged 5.7 million per individual (range: 2.2–14.5 million; single end).

Loci were assembled *de novo* in STACKS version 1.44, with the minimum reads required to create a stack as six (other settings left on default). Genotype and haplotype corrections in individual samples were then conducted using the STACKS *rxstacks* pipeline: loci for which 25% or more individuals had a confounded match to the catalogue were removed, excess haplotypes were pruned, sequencing errors were removed using the bounded model and single nucleotide polymorphisms (SNPs) were recalled, and catalogue loci with an average log likelihood less than -10.0 were removed (Rochette & Catchen, 2017). Following this, the catalogue of loci was rebuilt and each sample was mapped against it. The *export_sql.pl* function was used to generate a whitelist of loci containing one or two SNPs. Samples were filtered through the STACKS *populations* pipeline as a single population, with whitelisted loci retained if they were present in $\geq 75\%$ of samples, had a minimum individual stack depth of 10, a maximum observed heterozygosity of 0.5 and a minimum minor allele frequency of 0.05. After excluding technical replicates (following Mastretta-Yanes et al., 2015; Recknagel et al., 2015; genotyping error was $< 2.07\%$), and refiltering samples through STACKS *populations* (as before, but this time retaining a single SNP per locus), the final data set comprised 80 samples and 4,702 loci.

2.7 | Population genomics

RAXML (GTRCAT with 1,000 bootstrap replicates; Stamatakis, 2014) was run to check for phylogenetic clustering. Shared genetic ancestry was estimated using STRUCTURE (Pritchard, Stephens, & Donnelly, 2000) for 2–8 genetic clusters (K) implemented without population or phenotype priors using an admixture model, correlated allele frequencies and five iterations of 100,000 Markov chain Monte Carlo (MCMC) repetitions (10% burn-in). The best-fit value was determined using STRUCTURE HARVESTER (Earl & VonHoldt, 2012) to identify the highest ΔK (following Evanno, Regnaut, & Goudet, 2005). F_{ST} among sample sites and between colour morphs in sample sites 6 and 7 was calculated through pairwise differentiation tests in GENODIVE (Meirmans & van Tienderen, 2004); a post-hoc Bonferroni correction for multiple testing was applied to p -values using the *p.adjust* function in the R stats package (R Core Team, 2013).

2.8 | Gene expression

We used transcriptomic analyses to identify gene expression in yellow, brown and black skin. Skin samples from two locations (dorsal lateral and dorsal on stripe) per individual were taken from brown, yellow and striped salamanders (Figure S1b; $N = 3$ individuals per colour morph). Total RNA was extracted from ~ 25 mg of fresh tissue using the PureLink RNA Mini Kit, followed by a 4 mol/L lithium chloride precipitation at -20°C to remove contaminants. Library preparation, using polyA selection (TruSeq stranded mRNA kit), and 75 bp PE sequencing on the Illumina NextSeq 500 platform (RNA-Seq) was conducted at Glasgow Polyomics.

Raw read pairs ranged from 20.17 to 29.94 million per sample, with 86%–95% retained after quality filtering in TRIMMOMATIC version 0.36 (Bolger, Lohse, & Usadel, 2014). Raw reads were aligned to a draft reference *Salamandra* transcriptome assembly (TSA accession GIKK01000000; 44,165 transcripts; Goedbloed et al., 2017) using TOPHAT2 version 2.1.1 (Kim et al., 2013), and had an average alignment rate of 44.4%–48.9% when using default settings, but excluding mixed or discordant reads. Resulting SAM files were converted to BAM format using SAMTOOLS version 1.3.1 (Li et al., 2009), and hierarchical clustering of contigs was carried out using CORSET version 1.05 (default settings; Davidson & Oshlack, 2014). Differential gene expression analyses were conducted in DESEQ2 (Love, Huber, & Anders, 2014). This was done for pairwise comparisons of: (a) each colour combination: yellow versus black, yellow versus brown, and brown versus black; (b) between yellow and black skin in striped individuals only (quantifying intra-individual variation); and (c) between skin landmark 1 and skin landmark 2 across all individuals. Transcripts with an adjusted p -value of ≤ 0.1 were considered significantly differentially expressed (DE).

To identify the genes associated with DE transcripts, their sequence data were extracted from the reference assembly and searched against the NCBI nucleotide (BLASTN) and protein (BLASTX) databases (NCBI Resource Coordinators, 2017). Gene function and importance to animal coloration were then identified by searching available literature and databases, particularly UniProtKB (The UniProt Consortium, 2017), AMIGO 2 (Carbon et al., 2009), IMP (Integrative Multi-species Prediction; Wong, Krishnan, Yao, Tadych, & Troyanskaya, 2015) and the European Society for Pigment Cell Research (ESPCR) database (Montoliu, Oetting, & Bennett, 2017). Furthermore, gene ontology (GO) PANTHER Overrepresentation Tests (<http://geneontology.org/>; Ashburner et al., 2000; The Gene Ontology Consortium, 2015) were carried out to identify the biological processes, molecular functions and cellular components statistically overrepresented in those DE genes upregulated in different colours of skin (using *Homo sapiens*, *Anolis carolinensis*, *Danio rerio*, *Mus musculus* and *Xenopus tropicalis* gene sets as backgrounds in separate tests).

2.9 | Colour genomics

To reduce the impact of population structure on the inference of colour-associated loci across sampling sites, data for the 80 genotyped individuals used for population genetic analyses were re-filtered through STACKS *populations* as above, but without missing data constraints. We excluded sites deviating from Hardy–Weinberg equilibrium and containing more than 25% missing data across all individuals using VCFTOOLS, generating a data set of 2,149 SNP loci. Missing data (13.4%) were imputed using FASTPHASE version 1.4.8 (Scheet & Stephens, 2006) and SNP loci were converted into binary format using PLINK (Purcell et al., 2007). Genotypes were then corrected for population structure through linear regression with the first 10 PC scores from a PCA of the data in the R package *adegenet*.

Samples were striped ($N = 39$), yellow ($N = 24$) or brown ($N = 16$). Random forest (RF) analyses were conducted in R using the

randomForest package (Liaw & Wiener, 2002). Briefly, three independent analyses of 100,000 trees were run (ensuring a Pearson correlation coefficient of ≥ 0.95 between runs), which provided a mean permuted importance statistic (%IncMSE) for each SNP locus. The top 101 loci—roughly corresponding to the “upper end of the elbow” of the importance distribution, following Laporte et al. (2016)—were then subset and a backwards purging process used to determine the cohort that explained the highest amount of variance in the data. Briefly, three analyses of 10,000 trees were run, the mean r^2 across runs was calculated and the SNP with the smallest %IncMSE was removed. This was repeated until the data set contained only two SNP loci, with the iteration displaying the highest r^2 indicating the set of covarying loci best able to discriminate between colour morphs.

Latent factor mixed model (LFMM; Frichot, Schoville, Bouchard, & François, 2013) analyses were conducted in the R package *LEA* (Frichot & François, 2015). This package tests associations between loci and environmental (or phenotypic) gradients using an MCMC algorithm for regression analysis. The analysis was run 100 times, increasing the power to detect true associations, assuming one latent factor (K ; an exact value is not essential as it is estimated). Z-scores (the number of standard deviations above or below the population mean a data point is) from these runs were combined and the median value per locus calculated. The genomic inflation factor (λ) was then used to compute adjusted p -values for each locus. Finally, to correct for multiple testing, q -values were estimated for the adjusted p -values using the R package *qvalue*, with an false discovery rate (FDR) significance threshold of 0.1.

Loci identified by random forest and/or LFMM analyses were then identified, where possible. The only reference transcriptome or genome resource for salamanders is axolotl (*Ambystoma mexicanum*), a species that diverged ~151 million years ago from *Salamandra* (estimate from TimeTree.org). Therefore, direct search by BLAST was not informative because the sequence divergence is too high. Instead we used an indirect approach. The 60-bp candidate loci were searched against the Sal-site *A. mexicanum* transcripts database version 4.0 contigs (Keinath et al., 2015; Smith et al., 2005), which is largely unannotated. The contigs (80–3733 bp in length) to which the *Salamandra* loci accurately matched were used as query to search the NCBI BLASTN and BLASTX databases (<https://blast.ncbi.nlm.nih.gov/Blast.cgi>, default settings; contig, length and scores in Table S4). Gene function and importance to animal coloration were investigated as described for DE transcripts.

Finally, z-transformed F_{ST} (ZF_{ST}) was compared to delta genetic diversity ($\Delta\pi$) to identify loci putatively under selection between colour morphs (following Axelsson et al., 2013; Cagan & Blass, 2016). $\Delta\pi$ indicates if differentiation is driven by divergent selection or other background processes (i.e., low recombination). Compared to other processes, selection will reduce diversity in the morph under selection but not the alternative morph, thus leading to a $\Delta\pi$ that is different from zero. For this, per-site Weir and Cockerham's F_{ST} was calculated between all possible colour morph comparisons and colour morph-specific genetic diversity was calculated in *vcftools* for all variant sites; to mitigate population effects, this was carried out

using a subset of the data containing only individuals from the polymorphic sample sites 6 and 7. Per-site F_{ST} values were z-transformed and delta genetic diversity was calculated by taking the difference in diversity between colour morphs. We applied a $ZF_{ST} > 3$ as a threshold for detecting SNPs putatively under selection. This corresponds to SNPs with F_{ST} values above the 99.9th percentile of the empirical F_{ST} distribution or a p -value $< .0013$. As the ZF_{ST} is in units of standard deviations from the mean, it allows for a standardized identification of outlier SNPs. Those loci with a $ZF_{ST} \geq 3$, three standard deviations from the mean, were considered putatively under selection (following Axelsson et al., 2013; Cagan & Blass, 2016). Finally, a *STRUCTURE* analysis at $K = 3$ for visualization was carried out using just those loci identified as putatively under selection based on ZF_{ST} .

3 | RESULTS

3.1 | Colour morph differences

Objective quantification of colour pattern supported the grouping of individuals into the three colour categories: black-yellow striped, yellow morph, or brown morph (*Patternize* PC1 scores: $F_{(2, 217)} = 429.8$; $p < .005$; Figure 2a). Colour patterns did not differ between the sexes ($F_{(1, 218)} = 0.011$; $p = .916$) so data from males and females were combined. The three colour morphs differed in hue at the head, paratoid, dorsal and lateral landmarks (Table S1). Colour reflectance varied clearly across skin that was brown, yellow or black (Figure 2b); for example, the yellow on black-yellow striped individuals is the same yellow as on the yellow morph, and brown on the brown morph is similar to black on striped individuals (Table S1; Figure S2).

The types and densities of chromatophore cells in skin sections from dermal and epidermal layers at different colour landmarks were qualitatively different (Figure 2c). Based on visual inference, yellow skin had xanthophores, which are yellow-pigment-containing, in the epidermal layer and a high density of light-reflecting iridophores in the dermal layer. In poikilothermic skin, xanthophores contain yellow pigment while iridophores are structurally light-reflecting (Bagnara, 1972; Bagnara & Ferris, 1971; Bagnara, Frost, & Matsumoto, 1978; Kimura et al., 2014). In contrast, in both skin layers of brown and black skin only melanophores were evident, which are dark pigment-containing cells (Bagnara, 1972; Bagnara & Ferris, 1971; Bagnara et al., 1978; Mills & Patterson, 2009). The density of melanophores in the epidermal and the dermal layers was higher in the black than brown skin. In yellow skin, melanophores were infrequent and found as single cells or localized dermal clusters. These results demonstrate that yellow and black/brown skin colours are due to different underlying cellular structures.

3.2 | Population genomics

We tested for genome-wide population genetic differentiation between the different colour morphs based on 4,702 loci. We found

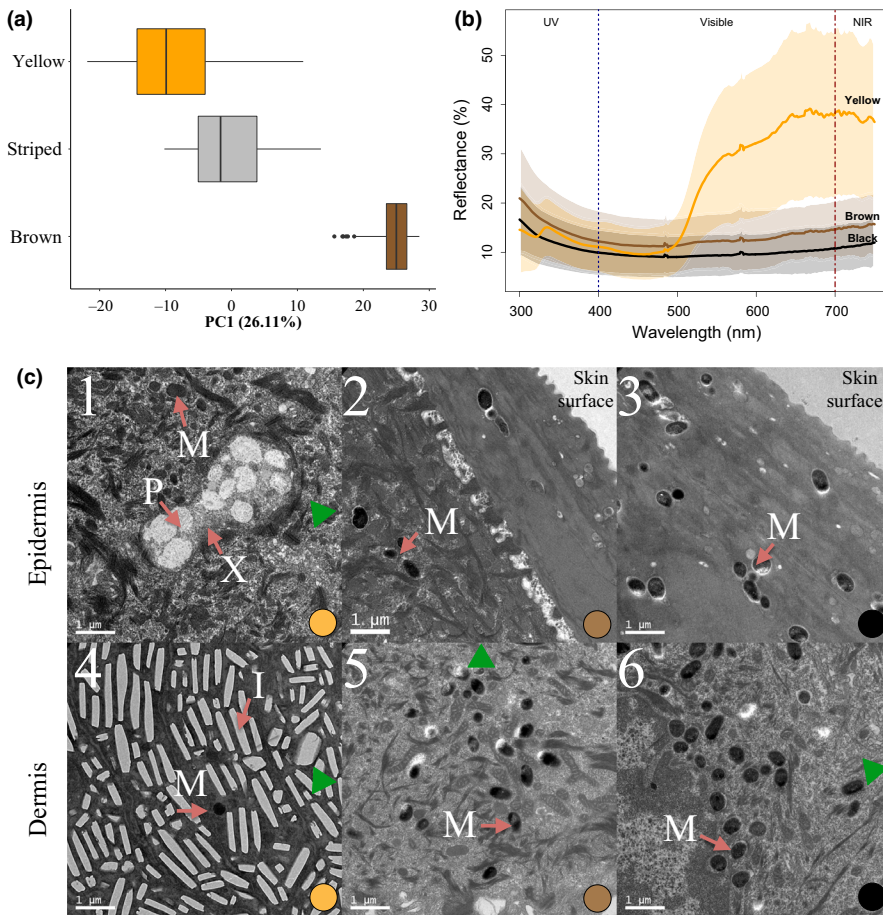


FIGURE 2 Colour phenotype characterization. (a) *Patternize* PC1 scores for salamanders after a priori assignment to colour morph ($n = 220$). (b) Average reflectance spectra of yellow ($n = 14$), brown ($n = 9$) and black ($n = 17$) skin across individuals (shading = standard deviation). (c) TEM images of *Salamandra* skin (circles in the bottom-right corner represent the skin colour): (1) TEM image of epidermal yellow skin from a striped salamander; (2) epidermal brown skin from a brown salamander; (3) epidermal black skin from a striped salamander; (4) dermal yellow skin from a striped salamander; (5) dermal brown skin from a brown salamander; (6) dermal black skin from a striped salamander. Cellular structures in C1–C6: P = pigment vesicle, M = melanophore, X = xanthophore, I = iridophore; green triangles point towards the external surface of the skin [Colour figure can be viewed at wileyonlinelibrary.com]

low but significant genetic differentiation between geographical localities regardless of colour (F_{ST} : 0.018–0.196, Table S3). Within the colour-polymorphic sample localities, there was no neutral genetic differentiation between colour morphs (all colour morph comparisons: $F_{ST} < 0.003$, $p > .12$; Table S2). Population clustering reflecting genomic proportions was driven by sample localities and not colour (Figure 3b). Individuals of different colours are intermixed in a maximum-likelihood (ML) tree and group into subclades by population (Figure 3a), as also evidenced in principal components (Figure S3). Overall these suggest no structuring by colour morph.

3.3 | Genotype–phenotype associations and functions

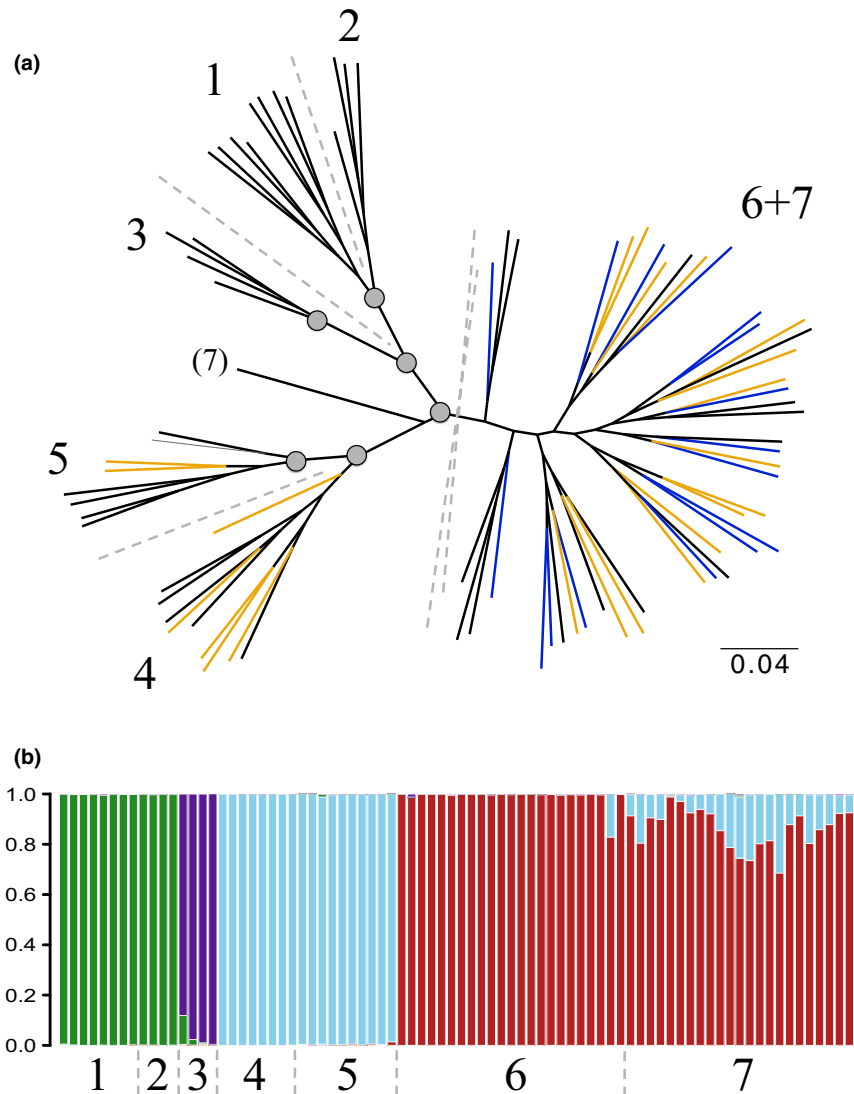
We tested for an association between genomic variation and phenotype and identified 21 loci best able to discriminate between individuals based on their colour morph using an RF analysis (61.22% variance explained; 2,149 loci in the data set; Figure S4a; Table 1). Five of these could be mapped indirectly via salamander contigs to vertebrate genes (Table S4): *BAZ2A*, *CAMK1*, *LDLRAD4*, *NYNRIN* and *TYR*. Using LFMM, we identified nine loci significantly correlated with coloration (q -value < 0.1 ; Table S4; Figure S4b), two of which mapped indirectly to genes: *prel* (protein preli-like) and *CAMK1*.

The functional relationships of the candidate coloration genes were explored in the Integrative Multi-species Prediction (IMP) platform. *TYR* had a clear functional link with colour, including known roles in pigmentation GO:0043473 (Probability, $Pr = 1$), melanin biosynthetic process GO:0042438 ($Pr = 1$) and iridophore differentiation GO:0050935 ($Pr = 0.059$; see Table S7 for a full list of colour-related processes identified). Potential roles were found for two other candidates. *CAMK1* is hypothesized to be involved in guanosine-related processes (GO:1901069, $Pr = 0.025$; GO:1901068, $Pr = 0.013$) in humans, guanosine being a key constituent of iridophores (Ide & Hama, 1972). *Prel* (protein preli-like) is a gene hypothesized to be involved in mouse pigmentation (IMP: gene *Prelid1*: GO:0043473, $Pr = 0.012$).

3.4 | Signals of selection

Through pairwise comparisons of genetic differentiation (ZF_{ST}) and genetic diversity, we identified 142 loci showing signals of response to selection between the three pairwise comparisons of colour morphs, namely increased genetic differentiation and decreased genetic diversity in one of the colour morphs (53 loci between yellow and striped, 55 loci between brown and striped, 55 loci between brown and yellow; Figure 4, cut-off at blue line; Table S5). Of these, 5–9 loci overlapped between pairwise comparisons (Table S5). No

FIGURE 3 Population genetic analysis of 4,702 ddRAD-Seq loci: (a) unrooted maximum clade credibility tree (RAxML) showing clustering by sample site not colour phenotype: yellow branches denote yellow salamanders, blue denote brown salamanders, and black denote black and yellow striped. Grey circles indicate branches with $\geq 85\%$ bootstrap support. (b) STRUCTURE plots for $K = 4$ (which has the highest ΔK), ordered by sample site (1–7) [Colour figure can be viewed at wileyonlinelibrary.com]



locus showed signals of selection in all three comparisons. Clustering based on outlier loci showed that colour grouping is highly consistent within individuals (Figure 4c).

Notably, the candidate *TYR* locus showed signals of selection and reduced genetic diversity in the yellow and brown morphs compared to the striped morph, and the candidate *CAMK1* locus showed signals of selection and reduced genetic diversity in the brown morph compared to both the yellow and the striped morphs. Additional loci under selection included one that mapped indirectly to the characterized gene *LDLRAD4* (Table S5).

Of all loci showing a signal of response to selection, 10 overlapped with those identified as being associated with coloration through genotype–phenotype association analyses (Table S5).

3.5 | Skin colour gene expression

Based on gene expression differences between skin of different colour, we identified a total of 167 DE genes (adjusted

p -value $< .1$; 180.8 million reads aligned to 35,926 reference transcripts) across all pairwise comparisons of yellow, brown and black skin (Figure 5). Specifically, the comparison of yellow and brown skin identified 95 DE transcripts annotated to 73 genes (Table S6; Figure S5); brown versus black skin identified 121 DE transcripts annotated to 94 unique genes (Table S6; Figure S6); and yellow versus black skin identified 42 DE transcripts annotated to 35 unique genes (Table S6; Figure S7). The striped individuals were sampled for yellow and black skin (one landmark each; Figure S1) and are within the latter comparison; those minimize confounding factors associated with interindividual variation and allow definitive identification of genes differentially expressed between colours.

Of all transcripts that were differentially expressed, 60 could be putatively associated with genes with known involvement in animal pigmentation through assessment by IMP, AMIGO 2 and literature searching (Table S7): 44 with melanophores, five with xanthophores, four with iridophores and 12 with other pigmentation-related processes (with some overlap, see Table S7 for full details).

TABLE 1 List of *de novo* loci that random forest and LFMM analyses inferred to be associated with colour morph, and putative gene IDs identified using the SAL-SITE assembly version 4.0 with NCBI BLAST

Analysis	Locus ID	Gene ID
LFMM	1731	<i>prel</i>
Random forest	2162	<i>TYR</i>
Random forest	7391	–
Random forest	10562	–
Random forest	11822	–
Random forest	12135	–
LFMM	15595	–
LFMM	16124	–
Random forest	16739	<i>LDLRAD4</i>
Random forest	21423	–
Random forest	22038	–
LFMM	24694	–
Random forest	27356	–
Random forest	28130	<i>CAMK1</i>
LFMM	28130	<i>CAMK1</i>
Random forest	32624	–
Random forest	32743	–
Random forest	36542	<i>BAZ2A</i>
LFMM	37375	–
Random forest	37821	–
LFMM	41341	–
LFMM	42961	–
Random forest	43841	–
Random forest	47160	–
Random forest	52344	–
Random forest	58978	–
Random forest	59960	–
LFMM	61782	–
Random forest	62160	<i>NYNRIN</i>
Random forest	84159	–

Notes: Locus 28130 is listed twice because it was independently identified in both analyses.

Based on over-representation analysis for genes up-regulated in skin of different colours, we identified molecular pathways putatively contributing to differences in expression (Table S8). Genes up-regulated in both brown and black skin compared to yellow skin included GO terms related to pigmentation, melanin biosynthesis and melanosomes. Broadly, genes up-regulated in yellow skin compared to black were associated with inosine and urate metabolic processes. None of the GO terms identified between brown and black skin have been associated previously with animal pigmentation. This suggests that the expression of brown and black skin may result from as yet uncharacterized molecular and cellular factors.

3.6 | Toxic secretions and colour polymorphism

We identified 18 metabolites in toxic secretions shared across most or all individuals (Table S9). A PCA of metabolite intensities for *S. s. bernardezi*, which indicates the relative abundance and variation, showed that the profiles of striped, yellow and brown salamanders overlapped along the first axis ($F_{(2,15)} = 0.219$; $p = .806$) but significantly separated along the second axis ($F_{(2,15)} = 5.595$; $p = .015$; Figure 6a).

Through a comparison with published data (Habermehl & Spiteller, 1967; Mebs & Pogoda, 2005), four of the 18 metabolites could be associated with known *Salamanca* alkaloids: cycloneosamandione (Peak02_375), samandarone (Peak07_375), samandarine (Peak19_417) and samandarine (Peak06_449; Figure 6b). The other 14 peaks represent currently uncharacterized compounds.

No significant differences were found in intensity between the colour morphs at either those four characterized alkaloids or at any of the 14 uncharacterized metabolites (Table S10; Figure 6b). There was a difference between the *S. s. bernardezi* (i.e., all three colour morphs combined) and the outgroup comparison *S. s. terrestris* at cycloneosamandione (Peak02_375), samandarone (Peak07_375) and samandarine (Peak06_449) (Table S10), which demonstrates the method is sensitive to variation and that these subspecies differed. Among the three colour morphs, some trends were evident, such as lower levels of samandarine in the yellow morph (one-way ANOVA: $F_{(2,15)} = 3.11$; $p = .074$). However, a large amount of variability was seen within and between the colour morphs (Figure 6b).

4 | DISCUSSION

4.1 | Molecular basis of colour in salamanders

Here we identified genomic loci associated with colour morph in these polymorphic salamanders that are yellow, brown or black-yellow striped. A total of 29 loci were inferred to covary with colour morph (21 from RF approaches and nine from LFMMs)—one locus overlapped across these complementary analyses (locus ID 28130 indirectly annotated to *CAMK1*). It is particularly striking that we inferred shared candidates across lines of analysis with transcriptomic and genomic data sets, and given the very large 34-Gb genome size of this species (Gregory, 2019), this suggests substantial regions in genetic linkage may underpin the genetic basis of colour in this species.

Although this is a nonmodel species with no reference genome, eight of those 29 colour-associated loci could be indirectly mapped to characterized genes by comparison with the biomedical model axolotl and other vertebrates. This included the colour gene *TYR*, which in mammals encodes the enzyme tyrosinase involved in the conversion of tyrosine into melanin pigments (Murisier & Beermann, 2006). Mutations in *TYR* have been shown to result in an albino phenotype in laboratory-reared axolotl salamanders (Woodcock et al., 2017), where melanophores develop but remain unmelanized (Frost, Epp, & Robinson, 1986). *TYR* is a particularly well-supported

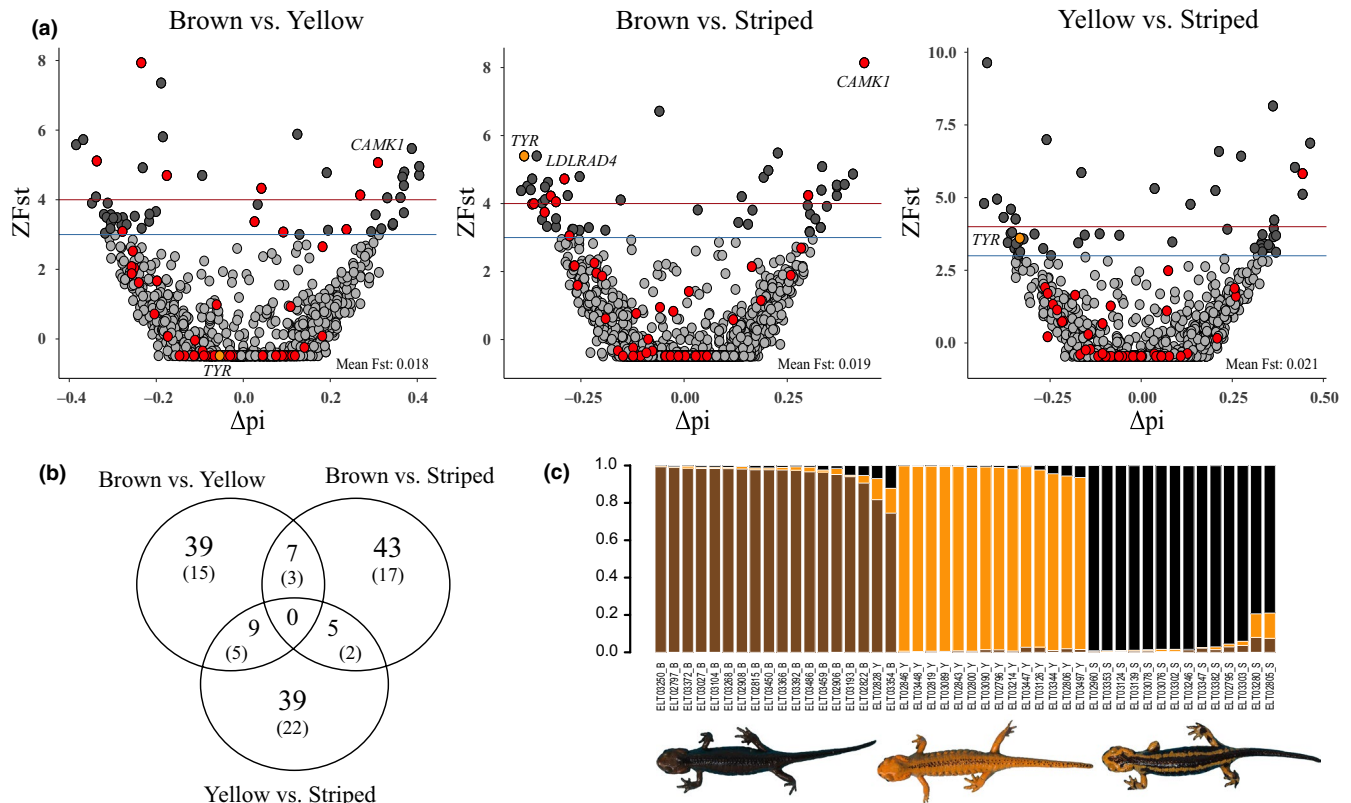


FIGURE 4 Genomic signals and response to selection within a colour polymorphic population based on 2,149 ddRAD-Seq loci. (a) Pairwise comparisons of z-transformed F_{ST} and genetic diversity between representative colour morphs: the blue line delimits a ZF_{ST} of three standard deviations from the mean, which we consider the cut-off (the red line is four standard deviations from the mean). Point shading groups loci by ZF_{ST} category: light grey <3 , dark grey >3 . Red points indicate those loci associated with colour phenotype identified across RF and LFMM analyses: labelled with a gene ID (where possible) if putatively under selection (the *TYR* loci is highlighted in orange in all cases). (b) Venn diagram showing the number of loci three (and four) standard deviations from the mean in each comparison. (c) A STRUCTURE plot ($K = 3$) of the 142 loci across comparisons with a $ZF_{ST} > 3$ standard deviations from the mean, showing clear clustering by colour morph [Colour figure can be viewed at wileyonlinelibrary.com]

candidate from several lines of evidence in our study; yellow skin also showed significantly reduced *TYR* expression in the transcriptome analyses and very few melanophores were seen in yellow skin through microscopy.

Several other candidates found to be significantly associated with colour morph also have biologically relevant links to coloration. For example, *BAZ2A* is known to share enhancers (GH12G055965 and GH12G056040) with the characterized colour gene *PEML* (premelanosome protein; Rebhan, Chalifa-Caspi, Prilusky, & Lancet, 1997). The gene *CAMK1* is hypothesized to be involved in guanosine-related processes in humans, with guanosine being a key constituent of iridophore cells (Ide & Hama, 1972). We found iridophore cells abundantly in the dermal layer of yellow *Salamandra* skin (Figure 2c). Revealingly, *CAMK1* was found to be associated with colour morph in the RF and the linear model analysis, suggesting it warrants further investigation for its role in this colour diversity. However, overall these candidates are somewhat tentative because of the lack of a closely related reference genome. Future work is needed to validate the loci for coloration.

Our findings from gene expression are more direct associations of colour morph and molecular bases and these supported several aspects of the genomics inference. Notably, the four most

down-regulated transcripts in yellow skin were related to three genes involved in melanin production (*PMEL*, *TRYP1* and *TYR*). Melanin-related genes were also important in distinguishing between yellow and brown skin, with the most up-regulated (*DEBF* family and *TFEC*) and down-regulated (*MAPK12*, *PMEL*, *MLANA*, *CCM2L* and *PDE1B*) genes in yellow skin all being melanin-process-related. Across vertebrates melanin is well established to be the main pigment of darker skin, fur and feather (Mills & Patterson, 2009). This strongly implicates melanin in the differences between yellow and dark (brown or black) skin in salamanders, consistent with our structural observations that melanophores are less abundant in yellow dermis (Figure 2c–4). The influence of melanin-pathway down-regulation compared to structural melanophore abundance in yellow skin warrants further study.

The seven transcripts most up-regulated in yellow skin compared to black skin mapped to genes with roles in pigmentation in vertebrates, including iridophore (*PNP* and *ADA2*), xanthophore (*PAX7* and *SLC2A11*) and leucophore (*SLC2A9*) production. Cells of the dermal chromatophore unit found in amphibian skin (Bagnara & Hadley, 1973) are either pigment-containing (yellow-red xanthophores) or structurally light-reflecting (iridophores). This unit is well known to exist in poikilothermic vertebrates (Bagnara, Taylor, & Hadley, 1968)

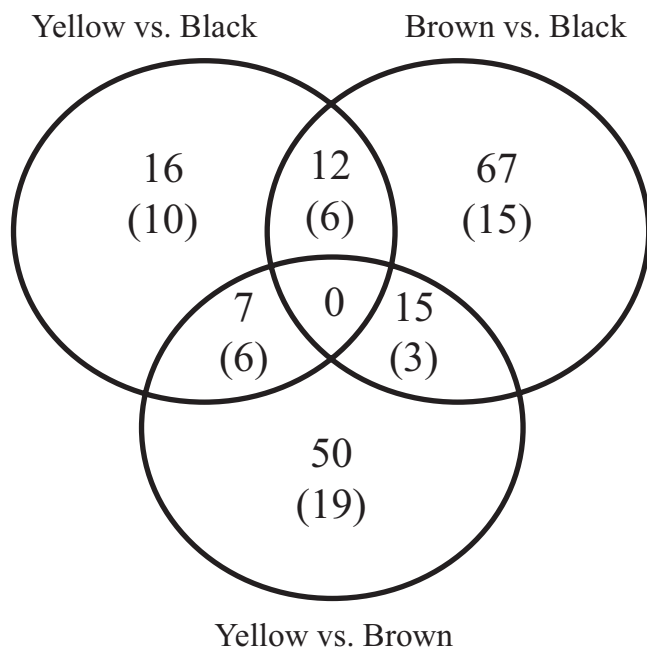


FIGURE 5 Venn diagram showing the number of significantly differentially expressed genes identified across all individuals in pairwise comparisons between the three skin colours (based on RNA-Seq data). Values in parentheses indicate the number of genes known to be associated with coloration

but to our knowledge its genetic basis has not been elucidated in amphibian skin. Here we have identified gene expression associated both with pigment (xanthophore) and structural (iridophore) components of yellow skin colour in salamanders.

The comparison between brown and black revealed a difference in gene expression levels, despite these two skin colours being similar in spectral reflectance and cellular structures. In total 24 genes differentially expressed between brown and black were associated with animal coloration: 19 of these are directly related to melanophores (five up-regulated and 14 down-regulated in brown skin). A further eight genes (*CIRBP*, *CYR61*, *MMP1*, *MMP3*, *AKR1C1*, *AKR1C3*, *TPBG* and *UPK1B*) are individually associated with GO terms relating to keratinocytes (Table S7). While the exact mechanisms remain unclear, it is known that keratinocytes interact with melanosomes either through melanin pigment transfer or uptake (Aspengren, Hedberg, & Wallin, 2006). Brown and black melanin pigments also share a common molecular basis, both being eumelanin polymers (Bagnara et al., 1978; Ito & Wakamatsu, 2011; Meredith & Sarna, 2006). Given this, we speculate that brown skin arises as a result of modifications in one or more melanin pathways, which either change the kinds or ratios of eumelanin pigments being produced in melanosomes. This would be consistent with recent studies on human skin pigmentation (Crawford et al., 2017; Ebanks et al., 2011) and could explain the cellular similarity, yet visual difference, between black and brown skin. Alternatively, the size and arrangement of melanophores in brown skin may be different to that in black skin, which could be elucidated by further quantitative studies on cellular structure.

In addition to specific genes, we found that higher level molecular pathways differed between the colour morphs. When compared to yellow skin, genes up-regulated in both brown and black skin included pigmentation-associated GO terms relating to melanin biosynthesis and melanosomes. Genes up-regulated in yellow skin compared to black were broadly associated with inosine and urate metabolic processes. This is functionally relevant because inosine is important in the production of xanthophores and iridophores (Krauss et al., 2013) and uric acid is important in the production of leucophores (Kimura et al., 2014). Our results suggest valuable insights into the biochemical pathways involved in chromatophore production, which remain poorly characterized (McLean, Lutz, Rankin, Stuart-Fox, & Moussalli, 2017) despite sharing some common developmental pathways with melanophores (see Beirl, Linbo, Cobb, & Cooper, 2014; Darias et al., 2013; Woodcock et al., 2017).

4.2 | Evidence colour is under selection?

Our findings from selection analyses give tentative insights into the mechanisms generating and maintaining this variation in colour and pattern. We identified 142 loci showing putative signals of response to selection between colour morphs. Several were shared across multiple pair-wise comparisons. Of the loci showing signals of response to selection, 10 overlapped with those associated with coloration through genotype–phenotype analyses (see Table S5). Such overlap lends support to the inference (Axelsson et al., 2013) and suggests a functional link between colour loci and targets of selection.

Four loci that are candidates for response to selection are particularly noteworthy because they are functionally related to colour in other organisms. First, the *CAMK1* locus showed decreased genetic diversity in both black-yellow striped and yellow salamanders compared to brown salamanders, suggesting that divergent selection is driving the differentiation between colour morphs in this locus. This is striking because based on our gene expression analysis we hypothesized that *CAMK1* is involved in iridophore production. *CAMK1* is involved in guanosine-related processes and guanosine is a key constituent in iridophores in frogs (Ide & Hama, 1972). These cells are found in yellow skin and apparently have been lost in brown individuals (Figure 2). As reduced genetic diversity in one morph compared to another can be indicative of a selective sweep (Wilson Sayres, Lohmueller, & Nielsen, 2014), this suggests that *CAMK1* may be under selection in some colour morphs. Furthermore, *CAMK1* was found in multiple association and selection analyses in this study, demonstrating a robust and consistent signal. These data suggest a functional link between the signals of selection we inferred and structural pigmentation, although the target and mechanism need to be resolved.

The *TYR* locus was also found to be putatively under selection between striped and yellow salamanders. It showed reduced genetic diversity in the derived yellow and brown morphs, suggesting that it is involved in colour pattern changes. Expression levels of *TYR*

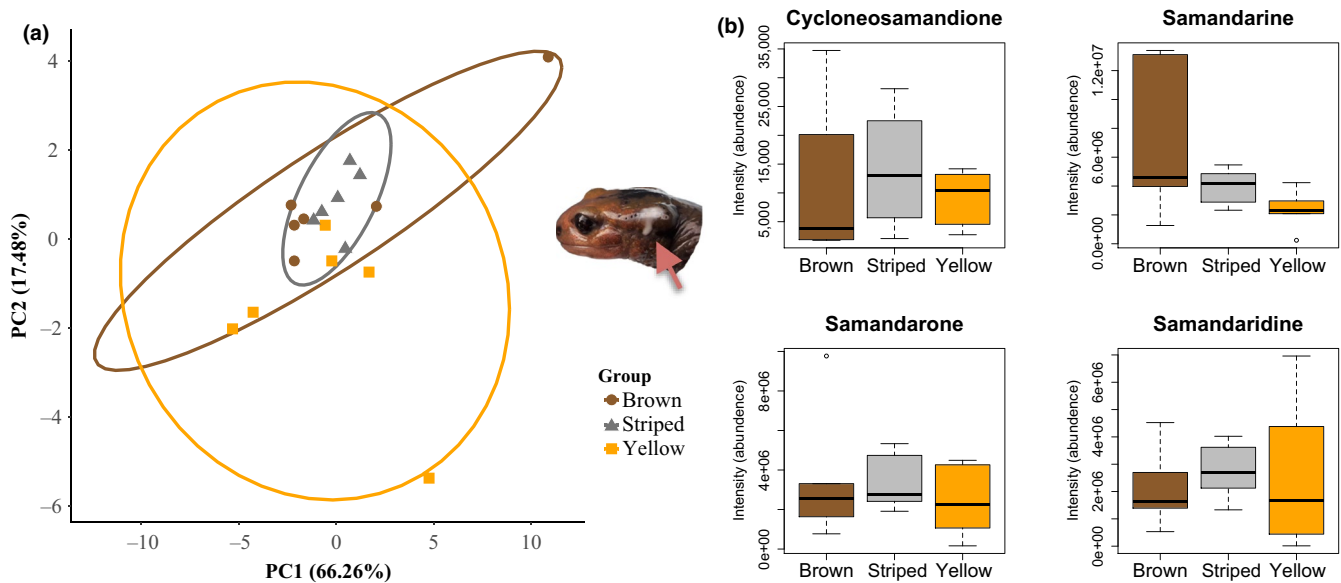


FIGURE 6 (a) PCA of 18 putative toxin metabolite intensities for yellow, brown and striped colour morphs. Inset: head with toxic secretion on the paratoid gland (red arrow). (b) Intensities for the four known *Salamandra* alkaloids across the three representative colour morphs; none differs significantly [Colour figure can be viewed at wileyonlinelibrary.com]

contribute towards coloration in other vertebrates, such as stripe formation in rodents (Mallarino et al., 2016) and grey versus black feather colorations in crows (Poelstra et al., 2014). Both of the derived salamander colour morphs—yellow and brown—are solid coloured and our findings suggest a possible role of TYR in the loss of stripes that warrants further testing.

4.3 | Ecological and evolutionary mechanisms of colour polymorphism

Post-hoc we can use the findings on phenotypes and genotypes to explore some standing hypotheses for the ecological and evolutionary drivers of amphibian colour pattern evolution: local adaptation to altitudinal differences, assortative mating or differential antipredator toxins (Beukema, Nicleza, et al., 2016; Beukema, Speybroeck, et al., 2016; Cott, 1940; Vences et al., 2014).

First, we do not find support for the hypothesis that the derived skin colour morph is adaptive for thermoregulation requirements at different altitudes, as had been suggested in other salamander lineages (Vences et al., 2014). We sampled salamanders from near sea level up to 1,312 m in the mountains and both the brown and the yellow colour morphs were always found alongside each other and were found at low to intermediate altitudes (172–679 m asl). In several locations all colour morphs that we studied were found together (Figure 1). This is in agreement with research spanning a broader distribution of *S. s. bernardezi* and niche breadths (Beukema, Nicleza, et al., 2016). Our finding suggests that the derived colour morphs are not differentially found at high or low altitudes at the spatial scale of this study, although historical effects and processes for altitudinal adaptation operating at the origin of different colour morphs cannot be ruled out.

Second, we do not find support for the hypothesis that there is contemporary reproductive isolation between colour morphs. Using comprehensive genome-wide markers we found that, within any colour polymorphic sample locality, there was no genetic differentiation between colour morphs. The lack of population genetic differentiation between colour morphs at genomic loci is in contrast to predictions; it had been suggested that these rare colour variants had a distinct history and previously were considered a separate subspecies (Beukema, Nicleza, et al., 2016; García-París, Alcobendas, Buckley, & Wake, 2003; Steinfartz et al., 2000). Our findings are also consistent with these derived yellow and brown morphs having arisen *in situ* within the ancestral black-yellow striped variant but without colour assortative mating. However, allopatric divergence followed by secondary contact with high gene flow between morphs cannot be ruled out. Future studies with colour-informed demographic modelling and outgroup sampling are required.

Third, we find equivocal support for a relationship between colour morph and the chemical profile of the famous toxic skin secretions of fire salamanders (Lüddecke et al., 2018; Mebs & Pogoda, 2005). Some differences are suggestive, such as in samandarine, and warrant further testing. Studies on other species and subspecies of *Salamandra* found no correlation between toxic secretions and colour pattern (Preißler et al., 2019; Sanchez et al., 2019; Vences et al., 2014) but these studies did not include the yellow or brown colour morphs. Colour in salamanders may therefore differ from amphibian systems where levels of conspicuousness and toxicity have been shown to be tightly correlated (Amézquita et al., 2017; Maan & Cummings, 2012). However, the sample size used for metabolomic analyses in the present study is limited and further research on toxicity and aposematism is needed.

Our investigations suggest we may need to consider new hypotheses for the generation and maintenance of colour variability in fire salamanders. The signals of selection found between these colour morphs do indicate a potentially adaptive role but in response to what selective pressure is not known. Definitively inferring the location and number of structural and regulatory changes underpinning the differences between salamander skin colour generation will require whole genome data and a well-annotated reference genome, something that is not currently available for *Salamandra* but will be valuable for more comprehensive testing.

5 | CONCLUSION

Our study identifies several molecular associations with coloration in polymorphic salamanders and suggests that these rare colour morphs are under selection. Natural admixture across colour morphs enabled us to analyse the association of population structure and coloration, without confounding background structure. The inferred genotype–phenotype associations, combined with an overlap of loci across different statistical approaches and genomic and transcriptomic data sets, enhances our confidence that we have in fact identified loci related to functional differences between colour morphs. These several lines of evidence from different 'omic data sets to known pigmentation genes, including *TYR*, *CAMK1* and *PMEL*, implicate a role in different colorations and suggest important candidate genes for future studies. We suggest that the current hypotheses are not sufficient to explain the ecological drivers of this distinctive and geographically restricted colour diversity. This research will facilitate studies on the evolution and convergence of colour patterns across vertebrates, which in turn will allow us to assess the consistency—as well as constraints on—vertebrate colour pattern evolution by natural selection.

ACKNOWLEDGMENTS

This research was supported by a Natural Environment Research Council PhD studentship (NE/L501918/1) to J.D.B. with K.R.E. and B.K.M., a Royal Society Research Grant (RG130800) to K.R.E., a Glasgow Natural History Society Blodwen Lloyd Binns Bequest grant to J.D.B., a Heredity Fieldwork Grant to K.R.E., a Wellcome Trust ISSF Catalyst Grant (Wellcome 105614/Z/14/Z) to K.R.E. and K.B., and a Spanish Ministry of Science Grant (CGL 2017-89898-R) to D.R.V. We are grateful to R. Williams, V. Ramos, M. Peso and G. Gallagher-Mackay for their aid during field sampling; to M. Mullin and M. Nokhbatolfighahai for their aid with TEM imaging; to A. Adam for her aid with laboratory work; to J. Galbraith and P. Herzyk at Glasgow Polyomics for sequencing; to H. Recknagel, M. Carruthers and E. Mittell for ongoing discussions and insights with the project; to A. Nolte and A. Rodriguez for access to unpublished reference transcriptomes; to M. Vences for advice on study design and critical comments on the manuscript; to R. Biek, R. MacLeod and M. Taylor for comments on an earlier draft of the study; to K. Schneider for bioinformatics advice; and to three anonymous reviewers for

constructive comments on the manuscript. We are grateful to the Dirección General de Recursos Naturales of the Principado de Asturias for field and collecting permits (number 2013/023669 and 2014/009413).



AUTHOR CONTRIBUTIONS

K.R.E., B.K.M., D.R.V., S.S. and J.D.B. designed the study. J.D.B., D.R.V. and K.R.E. collected samples. J.D.B. carried out the experimental work and analysis with involvement of A.J. (genomics), H.M.G. (transcriptomics) and K.B. and S.K.W. (metabolomics). K.B. and S.K.W. generated the GC-MS data. J.D.B. and K.R.E. wrote the manuscript. All authors contributed to the final version of the manuscript.

DATA AVAILABILITY STATEMENT

Sequence data are archived in the NCBI Sequence Read Archive under BioProject PRJNA606738 (RNA) and PRJNA610514 (DNA). SNP data sets and sequence alignment are archived in the freely accessible Univ. Glasgow Enlighten Repository <http://dx.doi.org/10.5525/gla.researchdata.982>.

ORCID

James D. Burgon  <https://orcid.org/0000-0002-7035-6614>
 David R. Vieites  <https://orcid.org/0000-0001-5551-7419>
 Arne Jacobs  <https://orcid.org/0000-0001-7635-5447>
 Stefan K. Weidt  <https://orcid.org/0000-0003-1127-9214>
 Helen M. Gunter  <https://orcid.org/0000-0002-6557-1993>
 Sebastian Steinfartz  <https://orcid.org/0000-0001-5347-3969>
 Karl Burgess  <https://orcid.org/0000-0002-0881-715X>
 Barbara K. Mable  <https://orcid.org/0000-0001-7118-4116>
 Kathryn R. Elmer  <https://orcid.org/0000-0002-9219-7001>

REFERENCES

- Acord, M. A., Anthony, C. D., & Hickerson, C.-A. M. (2013). Assortative mating in a polymorphic salamander. *Copeia*, 2013, 676.
- Alho, J. S., Herczeg, G., Söderman, F., Laurila, A., Jönsson, K. I., & Merilä, J. (2010). Increasing melanism along a latitudinal gradient in a wide-spread amphibian: Local adaptation, ontogenic or environmental plasticity? *BMC Evolutionary Biology*, 10, 317.
- Amézquita, A., Ramos, Ó., González, M. C., Rodríguez, C., Medina, I., Simões, P. I., & Lima, A. P. (2017). Conspicuousness, color resemblance, and toxicity in geographically diverging mimicry: The pan-Amazonian frog *Allobates femoralis*. *Evolution*, 71, 1039–1050.
- Andrade, P., Pinho, C., Pérez i de Lanuza, G., Afonso, S., Brejcha, J., Rubin, C.-J., ... Carneiro, M. (2019). Regulatory changes in pterin and carotenoid genes underlie balanced color polymorphisms in the wall lizard. *Proceedings of the National Academy of Sciences USA*, 116, 5633–5642.
- Andrews, S. (2010). FASTQC: A quality control tool for high throughput sequence data. <https://www.bioinformatics.babraham.ac.uk/projects/fastqc/>
- Ashburner, M., Ball, C. A., Blake, J. A., Botstein, D., Butler, H., Cherry, J. M., ... Sherlock, G. (2000). Gene Ontology: Tool for the unification of biology. *Nature Genetics*, 25, 25–29.
- Aspengren, S., Hedberg, D., & Wallin, M. (2006). Studies of pigment transfer between *Xenopus laevis* melanophores and fibroblasts in vitro and in vivo. *Pigment Cell Research*, 19, 136–145.

- Axelsson, E., Ratnakumar, A., Arendt, M.-L., Maqbool, K., Webster, M. T., Perloski, M., ... Lindblad-Toh, K. (2013). The genomic signature of dog domestication reveals adaptation to a starch-rich diet. *Nature*, 495, 360–364.
- Bagnara, J. T. (1972). Interrelationships of melanophores, iridophores, and xanthophores. In V. Riley (Ed.), *Pigmentation: Its genesis and biologic control* (pp. 171–180). New York, NY: Appleton-Century-Crofts.
- Bagnara, J. T., & Ferris, W. R. (1971). Interrelationship of chromatophores. In T. Kawamura, T. B. Fitzpatrick, & M. Seiji (Eds.), *Biology of the normal and abnormal melanocyte* (pp. 57–76). Tokyo, Japan: University of Tokyo.
- Bagnara, J. T., Frost, S. K., & Matsumoto, J. (1978). On the development of pigment patterns in amphibians. *American Zoologist*, 18, 301–312.
- Bagnara, J. T., & Hadley, M. E. (1973). *Chromatophores and color change: The comparative physiology of animal pigmentation*. Englewood Cliffs, NJ: Prentice-Hall.
- Bagnara, J. T., Taylor, J. D., & Hadley, M. E. (1968). The dermal chromatophore unit. *The Journal of Cell Biology*, 38, 67–79.
- Barrett, R. D. H., Laurent, S., Mallarino, R., Pfeifer, S. P., Xu, C. C. Y., Foll, M., ... Hoekstra, H. E. (2019). Linking a mutation to survival in wild mice. *Science*, 363, 499–504.
- Beirl, A. J., Linbo, T. H., Cobb, M. J., & Cooper, C. D. (2014). *oca2* regulation of chromatophore differentiation and number is cell type specific in zebrafish. *Pigment Cell & Melanoma Research*, 27, 178–189.
- Beukema, W., Nicieza, A. G., Lourenço, A., & Velo-Antón, G. (2016). Colour polymorphism in *Salamandra salamandra* (Amphibia: Urodela), revealed by a lack of genetic and environmental differentiation between distinct phenotypes. *Journal of Zoological Systematics and Evolutionary Research*, 54, 127–136.
- Beukema, W., Speybroeck, J., Velo-Antón, G., Eikermann, D., Rodríguez, A., Carranza, S., ... Al, E. (2016). Salamandra. *Current Biology*, 26, R696–R697.
- Bolger, A. M., Lohse, M., & Usadel, B. (2014). TRIMMOMATIC: A flexible trimmer for Illumina sequence data. *Bioinformatics*, 30, 2114–2120.
- Bonato, L., & Steinfartz, S. (2005). Evolution of the melanistic colour in the Alpine salamander *Salamandra atra* as revealed by a new subspecies from the Venetian Prealps. *Italian Journal of Zoology*, 72, 253–260.
- Cagan, A., & Blass, T. (2016). Identification of genomic variants putatively targeted by selection during dog domestication. *BMC Evolutionary Biology*, 16, 10.
- Cao, K.-A., Le, F., Rohart, I., Gonzalez, S., Dejean, B., Gautier, F., ... Liqueur, B. (2017). MIXOMICS: Omics data integration project. R package version 6.1.3. <https://CRAN.R-project.org/package=mixOmics>
- Carbon, S., Ireland, A., Mungall, C. J., Shu, S., Marshall, B., & Lewis, S. (2009). AMIGO: Online access to ontology and annotation data. *Bioinformatics*, 25, 288–289.
- Caro, T. (2005). The adaptive significance of coloration in mammals. *BioScience*, 55, 125–136.
- Catchen, J. M., Amores, A., Hohenlohe, P., Cresko, W., Postlethwait, J. H., & De Koning, D.-J. (2011). STACKS: building and genotyping loci de novo from short-read sequences. *G3*, 1, 171–182.
- Cott, H. (1940). *Adaptive colouration in animals*. London, UK: Methuen and Co.
- Crawford, N. G., Kelly, D. E., Hansen, M. E. B., Beltrame, M. H., Fan, S., Bowman, S. L., ... Tishkoff, S. (2017). Loci associated with skin pigmentation identified in African populations. *Science*, 358(6365), eaan8433. <https://doi.org/10.1126/science.aan8433>
- Darias, M. J., Andree, K. B., Boglino, A., Fernández, I., Estévez, A., & Gisbert, E. (2013). Coordinated regulation of chromatophore differentiation and melanogenesis during the ontogeny of skin pigmentation of *Solea senegalensis* (Kaup, 1858). *PLoS ONE*, 8, e63005.
- Davidson, N. M., & Oshlack, A. (2014). Corset: Enabling differential gene expression analysis for de novo assembled transcriptomes. *Genome Biology*, 15, 410.
- Duellman, W. E., & Trueb, L. (1994). *Biology of amphibians*. London, UK: The John Hopkins University Press.
- Earl, D. A., & VonHoldt, B. M. (2012). STRUCTURE HARVESTER: A website and program for visualizing STRUCTURE output and implementing the Evanno method. *Conservation Genetics Resources*, 4, 359–361.
- Ebanks, J. P., Koshoffer, A., Wickett, R. R., Schwemberger, S., Babcock, G., Hakozi, T., & Boissy, R. E. (2011). Epidermal keratinocytes from light vs. dark skin exhibit differential degradation of melanosomes. *Journal of Investigative Dermatology*, 131, 1226–1233.
- Evanno, G., Regnaut, S., & Goudet, J. (2005). Detecting the number of clusters of individuals using the software STRUCTURE: A simulation study. *Molecular Ecology*, 14, 2611–2620.
- Frichot, E., & François, O. (2015). LEA: An R package for landscape and ecological association studies. *Methods in Ecology and Evolution*, 6, 925–929.
- Frichot, E., Schoville, S. D., Bouchard, G., & François, O. (2013). Testing for associations between loci and environmental gradients using latent factor mixed models. *Molecular Biology and Evolution*, 30, 1687–1699.
- Frost, S. K., Epp, L. G., & Robinson, S. J. (1986). The pigmentary system of developing axolotls. *Journal of Embryology and Experimental Morphology*, 92, 255–268.
- García-París, A. M., Alcobendas, M., Buckley, D., & Wake, D. B. (2003). Dispersal of viviparity across contact zones in Iberian populations of fire salamanders (*Salamandra*) inferred from discordance of genetic and morphological traits. *Evolution*, 57, 129–143.
- Goedbloed, D. J., Cypionka, T., Altmüller, J., Rodríguez, A., Küpfer, E., Segev, O., ... Steinfartz, S. (2017). Parallel habitat acclimatization is realized by the expression of different genes in two closely related salamander species (genus *Salamandra*). *Heredity (Edinb)*, 119(6), 429–437.
- Gordon, A., & Hannon, G. J. (2008). Fastx-toolkit: fastx_barcode_splitter.pl. http://hannonlab.cshl.edu/fastx_toolkit/
- Graham, L., & Orenstein, J. M. (2007). Processing tissue and cells for transmission electron microscopy in diagnostic pathology and research. *Nature Protocols*, 2, 2439–2450.
- Gregory, T. R. (2019). Animal genome size database. <http://www.genomesize.com>.
- Habermehl, G., & Spiteller, G. (1967). Massenspektren der Salamander-Alkaloide. *Justus Liebigs Annalen Der Chemie*, 706, 213–222.
- Harris, R. B., Irwin, K., Jones, M. R., Laurent, S., Barrett, R. D. H., Nachman, M. W., ... Pfeifer, S. P. (2020). The population genetics of crypsis in vertebrates: Recent insights from mice, hares, and lizards. *Heredity*, 124(1), 1–14. <https://doi.org/10.1038/s41437-019-0257-4>
- Hoffman, E. A., & Blouin, M. S. (2000). A review of colour and pattern polymorphisms in anurans. *Biological Journal of the Linnean Society*, 70, 633–665.
- Hubbard, J. K., Uy, J. A. C., Hauber, M. E., Hoekstra, H. E., & Safran, R. J. (2010). Vertebrate pigmentation: From underlying genes to adaptive function. *Trends in Genetics*, 26, 231–239.
- Ide, H., & Hama, T. (1972). Guanine formation in isolated iridophores from bullfrog tadpoles. *Biochimica Et Biophysica Acta (BBA) - General Subjects*, 286, 269–271.
- Ito, S., & Wakamatsu, K. (2011). Diversity of human hair pigmentation as studied by chemical analysis of eumelanin and pheomelanin. *Journal of the European Academy of Dermatology and Venereology*, 25, 1369–1380.
- Keinath, M. C., Timoshevskiy, V. A., Timoshevskaya, N. Y., Tsonis, P. A., Voss, S. R., & Smith, J. J. (2015). Initial characterization of the large genome of the salamander *Ambystoma mexicanum* using shotgun and laser capture chromosome sequencing. *Scientific Reports*, 5, 16413.
- Kerr, J. G. (1919). "Camouflage" of ships in war. *Nature*, 103, 204–205.
- Kim, D., Pertea, G., Trapnell, C., Pimentel, H., Kelley, R., & Salzberg, S. L. (2013). TopHat2: Accurate alignment of transcriptomes in the presence of insertions, deletions and gene fusions. *Genome Biology*, 14, R36.

- Kimura, T., Nagao, Y., Hashimoto, H., Yamamoto-Shiraishi, Y., Yamamoto, S., Yabe, T., ... Naruse, K. (2014). Leucophores are similar to xanthophores in their specification and differentiation processes in medaka. *Proceedings of the National Academy of Sciences USA*, 111, 7343–7348.
- Koepfli, K.-P., Paten, B., & O'Brien, S. J. (2015). The Genome 10K Project: A way forward. *Annual Review of Animal Biosciences*, 3, 57–111.
- Köhler, G., & Steinfartz, S. (2006). A new subspecies of the fire salamander, *Salamandra salamandra* (Linnaeus, 1758) from the Tendi valley, Asturias, Spain. *Salamandra*, 42, 13–20.
- Krauss, J., Astrinidis, P., Astrinides, P., Frohnhöfer, H. G., Walderich, B., & Nüsslein-Volhard, C. (2013). transparent, a gene affecting stripe formation in Zebrafish, encodes the mitochondrial protein Mpv17 that is required for iridophore survival. *Biology Open*, 2, 703–710.
- Kusche, H., Elmer, K. R., & Meyer, A. (2015). Sympatric ecological divergence associated with a color polymorphism. *BMC Biology*, 13, 82.
- Laporte, M., Pavey, S. A., Rougeux, C., Pierron, F., Lauzent, M., Budzinski, H., ... Bernatchez, L. (2016). RAD sequencing reveals within-generation polygenic selection in response to anthropogenic organic and metal contamination in North Atlantic Eels. *Molecular Ecology*, 25, 219–237.
- Li, H., Handsaker, B., Wysoker, A., Fennell, T., Ruan, J., Homer, N., ... 1000 Genome Project Data Processing Subgroup. (2009). The Sequence Alignment/Map format and SAMtools. *Bioinformatics*, 25, 2078–2079.
- Liaw, A., & Wiener, M. (2002). Classification and regression by random Forest. *R News*, 2, 18–22.
- Love, M. I., Huber, W., & Anders, S. (2014). Moderated estimation of fold change and dispersion for RNA-seq data with DESeq2. *Genome Biology*, 15, 550.
- Lüddecke, T., Schulz, S., Steinfartz, S., & Vences, M. (2018). A salamander's toxic arsenal: Review of skin poison diversity and function in true salamanders, genus *Salamandra*. *The Science of Nature*, 105, 56.
- Maan, M. E., & Cummings, M. E. (2012). Poison frog colors are honest signals of toxicity, particularly for bird predators. *The American Naturalist*, 179, E1–14.
- Maia, R., Eliason, C. M., Bitton, P.-P., Doucet, S. M., & Shawkey, M. D. (2013). PAVO: An R package for the analysis, visualization and organization of spectral data. *Methods in Ecology and Evolution*, 4, 906–913.
- Mallarino, R., Henegar, C., Mirasierra, M., Manceau, M., Schradin, C., Vallejo, M., ... Hoekstra, H. E. (2016). Developmental mechanisms of stripe patterns in rodents. *Nature*, 539, 518–523.
- Mastretta-Yanes, A., Arrigo, N., Alvarez, N., Jorgensen, T. H., Piñero, D., & Emerson, B. C. (2015). Restriction site-associated DNA sequencing, genotyping error estimation and de novo assembly optimization for population genetic inference. *Molecular Ecology Resources*, 15(1), 28–41. <https://doi.org/10.1111/1755-0998.12291>
- McCartney-Melstad, E., Mount, G. G., & Shaffer, H. B. (2016). Exon capture optimization in amphibians with large genomes. *Molecular Ecology Resources*, 16, 1084–1094.
- McLean, C. A., Lutz, A., Rankin, K. J., Stuart-Fox, D., & Moussalli, A. (2017). Revealing the biochemical and genetic basis of color variation in a polymorphic lizard. *Molecular Biology and Evolution*, 34, 1924–1935.
- Mebs, D., & Pogoda, W. (2005). Variability of alkaloids in the skin secretion of the European fire salamander (*Salamandra salamandra terrestris*). *Toxicon*, 45, 603–606.
- Meirmans, P. G., & van Tienderen, P. H. (2004). genotype and genodive: Two programs for the analysis of genetic diversity of asexual organisms. *Molecular Ecology Notes*, 4, 792–794.
- Meredith, P., & Sarna, T. (2006). The physical and chemical properties of eumelanin. *Pigment Cell Research*, 19, 572–594.
- Mills, M. G., & Patterson, L. B. (2009). Not just black and white: Pigment pattern development and evolution in vertebrates. *Seminars in Cell & Developmental Biology*, 20, 72–81.
- Montoliu, L., Oetting, W. S., & Bennett, D. C. (2017). European Society for Pigment Cell Research – Color Genes. <http://www.espcr.org/micemut/>
- Moore, J. D., & Ouellet, M. (2015). Questioning the use of an amphibian colour morph as an indicator of climate change. *Global Change Biology*, 21, 566–571.
- Murisier, F., & Beermann, F. (2006). Genetics of pigment cells: Lessons from the tyrosinase gene family. *Histology and Histopathology*, 21, 567–578.
- NCBI Resource Coordinators (2017). Database Resources of the National Center for Biotechnology Information. *Nucleic Acids Research*, 45, D12–D17.
- Nowoshilow, S., Schloissnig, S., Fei, J. F., Dahl, A., Pang, A. W. C., Pippel, M., ... Myers, E. W. (2018). The axolotl genome and the evolution of key tissue formation regulators. *Nature*, 554(7690), 50–55. <https://doi.org/10.1038/nature25458>
- Peterson, B. K., Weber, J. N., Kay, E. H., Fisher, H. S., & Hoekstra, H. E. (2012). Double digest RADseq: An inexpensive method for de novo SNP discovery and genotyping in model and non-model species. *PLoS ONE*, 7, e37135.
- Poelstra, J. W., Vijay, N., Bossu, C. M., Lantz, H., Ryll, B., Müller, I., ... Wolf, J. B. W. (2014). The genomic landscape underlying phenotypic integrity in the face of gene flow in crows. *Science*, 344, 1410–1414.
- Preißler, K., Gippner, S., Lüddecke, T., Krause, E. T., Schulz, S., Vences, M., & Steinfartz, S. (2019). More yellow more toxic? Sex rather than alkaloid content is correlated with yellow coloration in the fire salamander. *Journal of Zoology*, 308(4), 293–300.
- Pritchard, J. K., Stephens, M., & Donnelly, P. (2000). Inference of population structure using multilocus genotype data. *Genetics*, 155, 945–959.
- Purcell, S., Neale, B., Todd-Brown, K., Thomas, L., Ferreira, M. A. R., Bender, D., ... Sham, P. C. (2007). PLINK: A tool set for whole-genome association and population-based linkage analyses. *The American Journal of Human Genetics*, 81, 559–575.
- R Core Team. (2013). *A language and environment for statistical computing*. Vienna, Austria: Foundation for Statistical Computing. <http://www.r-project.org/>
- Rebhan, M., Chalifa-Caspi, V., Prilusky, J., & Lancet, D. (1997). GENECARDS: Integrating information about genes, proteins and diseases. *Trends in Genetics*, 13, 163.
- Recknagel, H., Jacobs, A., Herzyk, P., & Elmer, K. R. (2015). Double-digest RAD sequencing using Ion Proton semiconductor platform (ddRAD-seq-ion) with nonmodel organisms. *Molecular Ecology Resources*, 15, 1316–1329.
- Rochette, N. C., & Catchen, J. M. (2017). Deriving genotypes from RAD-seq short-read data using Stacks. *Nature Protocols*, 12, 2640–2659.
- Rodríguez, A., Burgon, J. D. J. D., Lyra, M., Irisarri, I., Baurain, D., Blaustein, L., ... Vences, M. (2017). Inferring the shallow phylogeny of true salamanders (*Salamandra*) by multiple phylogenomic approaches. *Molecular Phylogenetics and Evolution*, 115, 16–26.
- Rudh, A., & Qvarnström, A. (2013). Adaptive colouration in amphibians. *Seminars in Cell and Developmental Biology*, 24, 553–561.
- Ruxton, G. D., Sherratt, T. N., & Speed, M. P. (2004). *Attack: The evolutionary ecology of crypsis, warning signals and mimicry*. Oxford, UK: Oxford University Press.
- Sanchez, E., Pröhl, H., Lüddecke, T., Schulz, S., Steinfartz, S., & Vences, M. (2019). The conspicuous postmetamorphic coloration of fire salamanders, but not their toxicity, is affected by larval background albedo. *Journal of Experimental Zoology Part B: Molecular and Developmental Evolution*, 332(1–2), 26–35.
- Scheet, P., & Stephens, M. (2006). A fast and flexible statistical model for large-scale population genotype data: Applications to inferring missing genotypes and haplotypic phase. *The American Journal of Human Genetics*, 78(7), 629–644.
- Smith, J. J., Putta, S., Walker, J. A., Kump, D. K., Samuels, A. K., Monaghan, J. R., ... Voss, S. R. (2005). Sal-Site: Integrating new and existing ambystomatid salamander research and informational resources. *BMC Genomics*, 6, 181.

- Sparreboom, M., & Arntzen, J. W. (2014). *Salamanders of the Old World: The Salamanders of Europe, Asia and Northern Africa*. Zeist, The Netherlands: KNNV Publishing.
- Stamatakis, A. (2014). RAXML version 8: A tool for phylogenetic analysis and post-analysis of large phylogenies. *Bioinformatics*, 30, 1312–1313.
- Steinfartz, S., Veith, M., & Tautz, D. (2000). Mitochondrial sequence analysis of *Salamandra* taxa suggests old splits of major lineages and postglacial recolonizations of Central Europe from distinct source populations of *Salamandra salamandra*. *Molecular Ecology*, 9, 397–410.
- Stevens, M., & Ruxton, G. D. (2012). Linking the evolution and form of warning coloration in nature. *Proceedings of the Royal Society B: Biological Sciences*, 279, 417–426.
- Stuart-Fox, D., & Moussalli, A. (2009). Camouflage, communication and thermoregulation: Lessons from colour changing organisms. *Philosophical Transactions of the Royal Society of London. Series B, Biological Sciences*, 364, 463–470.
- Thayer, A. (1909). *Concealing coloration in the animal kingdom*. New York, NY: Macmillan.
- The Gene Ontology Consortium. (2015). Gene Ontology Consortium: Going forward. *Nucleic Acids Research*, 43, D1049–D1056.
- The UniProt Consortium (2017). UniProt: The universal protein knowledgebase. *Nucleic Acids Research*, 45, D158–D169.
- Thiesmeier, B. (2004). *Der Feuersalamander*. Bielefeld, Germany: Laurenti publishing house.
- Thorn, R., & Raffaëlli, J. (2001). *Les salamandres de l'ancien monde*. Paris, France: Boubée.
- Trochet, A., Moulherat, S., Calvez, O., Stevens, V. M., Clobert, J., & Schmeller, D. S. (2014). A database of life-history traits of European amphibians. *Biodiversity Data Journal*, 2, e4123.
- Van Belleghem, S. M., Papa, R., Ortiz-Zuazaga, H., Hendrickx, F., Jiggins, C. D., Owen McMillan, W., & Counterman, B. A. (2018). PATTERNIZE: An R package for quantifying colour pattern variation. *Methods in Ecology and Evolution*, 9(2), 390–398. <https://doi.org/10.1111/2041-210X.12853>
- Vences, M., Galán, P., Vieites, D. R., Puente, M., Oetter, K., & Wanke, S. (2002). Field body temperatures and heating rates in a montane frog population: The importance of black dorsal pattern for thermoregulation. *Annales Zoologici Fennici*, 39, 209–220.
- Vences, M., Sanchez, E., Hauswaldt, J. S., Eikermann, D., Rodríguez, A., Carranza, S., ... Steinfartz, S. (2014). Nuclear and mitochondrial multilocus phylogeny and survey of alkaloid content in true salamanders of the genus *Salamandra* (Salamandridae). *Molecular Phylogenetics and Evolution*, 73, 208–216.
- Wilson Sayres, M. A., Lohmueller, K. E., & Nielsen, R. (2014). Natural selection reduced diversity on human Y chromosomes. *PLoS Genetics*, 10(1), e1004064. <https://doi.org/10.1371/journal.pgen.1004064>
- Wong, A. K., Krishnan, A., Yao, V., Tadych, A., & Troyanskaya, O. G. (2015). IMP 2.0: A multi-species functional genomics portal for integration, visualization and prediction of protein functions and networks. *Nucleic Acids Research*, 43, W128–W133.
- Woodcock, M. R., Vaughn-Wolfe, J., Elias, A., Kump, D. K., Kendall, K. D., Timoshevskaya, N., ... Voss, S. R. (2017). Identification of mutant genes and introgressed tiger salamander DNA in the laboratory axolotl, *Ambystoma mexicanum*. *Scientific Reports*, 7, 6.

SUPPORTING INFORMATION

Additional supporting information may be found online in the Supporting Information section.

How to cite this article: Burgon JD, Vieites DR, Jacobs A, et al. Functional colour genes and signals of selection in colour-polymorphic salamanders. *Mol Ecol*. 2020;29:1284–1299. <https://doi.org/10.1111/mec.15411>